Performance of a Doppler-Aided GPS Navigation System for Aviation Applications under Ionospheric Scintillation

Tsung-Yu Chiou, Jiwon Seo, Todd Walter, and Per Enge,
Stanford University, Palo Alto, CA

BIOGRAPHY

Tsung-Yu Chiou is a Ph.D. candidate in the Aeronautics and Astronautics Department at Stanford University. He received his B.S. in Aerospace Engineering in 1998 from Tamkang University, Taiwan and his M.S. from Stanford in 2002. His research currently focuses on the performance analysis and validation of Doppler-aided GPS carrier-tracking loops. He is also looking into the solutions to the problem of GPS/WAAS performance degradation caused by ionospheric scintillation.

Jiwon Seo is a Ph.D. candidate in Aeronautics and Astronautics at Stanford University. He received his B.S. in Aerospace Engineering from KAIST (Korea Advanced Institute of Science and Technology) and received M.S. degrees in Aeronautics and Astronautics, Electrical Engineering from Stanford. He was a recipient of Samsung Lee Kun Hee Graduate Fellowship for five years. His current research focuses on aircraft navigation using GPS and WAAS under severe ionospheric scintillation of the equatorial region.

Dr. Todd Walter received his B.S. in physics from Rensselaer Polytechnic Institute and his Ph.D. in 1993 from Stanford University. He is currently a Senior Research Engineer at Stanford University. He is a co-chair of the WAAS Integrity Performance Panel (WIPP) that focuses on the implementation of WAAS and the development of its later stages. Key contributions include: early prototype development proving the feasibility of WAAS, significant contribution to MOPS design and validation, co-editing of the Institute of Navigation's book of papers about WAAS and its European and Japanese counterparts, and design of ionospheric algorithms for WAAS. He was the co-recipient of the 2001 ION early achievement award.

Dr. Per Enge is a Professor of Aeronautics and Astronautics at Stanford University, where he is the Kleiner-Perkins, Mayfield, Sequoia Capital Professor in the School of Engineering. He directs the GPS Research Laboratory, which develops satellite navigation systems based on the Global Positioning System (GPS). These navigation systems augment GPS to improve accuracy and provide real time error bounds. Professor Enge's research focuses on the design of navigation systems which satisfy stringent requirements with respect to accuracy, integrity (truthfulness), time availability, and continuity. Enge has received the Kepler, Thurlow and Burka Awards from the Institute of Navigation (ION) for his work. He is also a Fellow of the ION and the Institute of Electrical and Electronics Engineers (IEEE). He received his PhD from the University of Illinois in 1983, where he designed a direct-sequence multiple-access communication system that provided an orthogonal signal set to each user.

ABSTRACT

Aircraft landing using the Global Positioning System (GPS) in equatorial regions is more difficult than in other regions because ionospheric scintillation is prevalent. Ionospheric scintillation causes amplitude fades of 20 dB or more and an increase in the phase jitter.

This research evaluates techniques to enhance a GPS receiver for overcoming ionospheric scintillation. To validate the designed GPS receiver, a GPS channel model for aircraft landing in equatorial regions is built based on the use of high fidelity GPS constellation simulator, clock emulator, and real ionosphere interfered with GPS data collected in an equatorial region.

The results of this research demonstrate that the integration of a GPS receiver with a low-cost inertial navigation system provides the capability to operate continuously during the periods of strong scintillation. In addition, so-called vector processing also shows promise for less severe scintillation environment. Various combinations of receiver tracking architectures and aiding

methods have been conducted to quantify the sensitivity improvement of an "aided" GPS receiver.

1. INTRODUCTION

This work designs a Doppler-aided GPS navigation system for processing weak signals caused by ionospheric scintillation. The relative motion between the satellite and the receiver causes a Doppler shift in the GPS signals. Doppler-aiding means that we want to provide the Doppler estimate to the GPS receiver beforehand. By doing so, we release the loadings of a GPS receiver such that it has more capability of dealing with weak signals.

Figure 1 reveals our motivation for this work and the three major challenges to the GPS receiver used for the considered scenario. We investigate the difficulties of aircraft landing using a GPS in equatorial regions. The ionospheric scintillation is more severe in equatorial regions than in other regions. Therefore, the first challenge of the GPS receiver is the weak signals due to scintillation. However, the weak signal condition due to scintillation is not the only challenge. The GPS receiver clock, a crystal oscillator, is sensitive to the aircraft vibration. Because of the impact of this vibration on the GPS receiver clock, the phase noise in the GPS carrier tracking loop increases. Furthermore, disturbances such as wind gusts and a pilot's maneuvers create dynamic stress to the GPS receiver. As a result, the GPS receiver for aircraft landing in equatorial regions must overcome the aforementioned three challenges.

The governing concept for the design of a GPS receiver to surmount the three challenges is determining the bandwidth of the carrier tracking loop inside the GPS receiver. In principle, we seek a way to assist the GPS receiver in reducing the bandwidth for better noise suppression. However, as presented in Figure 1, a higher bandwidth of the carrier tracking loop is required to track the clock dynamics as well as the platform dynamics. Hence, this is a trade-off study focused on the bandwidth of the GPS receiver. To evaluate the performance of the designed GPS receiver for the concerned application under strong scintillation conditions, we have conducted the following analyses and implementations to assess the performance of the designed receiver.

1. To have high-fidelity GPS radio frequency (RF) data, we have built a realistic channel model for aircraft landing using a GPS in a strong scintillation environment.
2. We have designed a GPS receiver which runs coherent and non-coherent tracking in parallel and have evaluated the performance of both tracking architectures.
3. The technique of Doppler-aiding is applied to both coherent and non-coherent tracking architectures.
4. Two Doppler-aiding sources are considered. The first technique is vector processing [1], and the second technique is tightly-coupled GPS/INS integration.

The remainder of the paper elaborates the aforementioned items in detail.

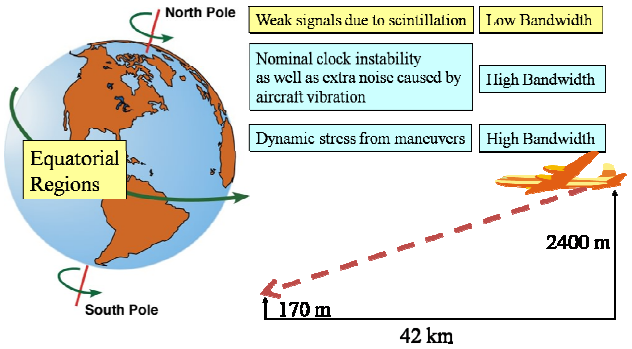

Figure 1: Challenges of Aircraft Landing Using GPS in Equatorial Regions

2. CHANNEL MODELING

This section demonstrates the processes used to build the channel model for aircraft landing using a GPS under strong scintillation conditions. By building the channel model, a realistic GPS RF signal for the considered conditions is obtained. The channel model includes strong ionospheric scintillation, vibration effects on the receiver clock, and aircraft platform dynamics.

2.1 Ionospheric Scintillation

Ionospheric scintillation is caused by local ionosphere plasma anomalies. The process of electron-ion recombination after sunset is not uniform. Therefore patches containing irregular electron density are formed. If the GPS signal passes through these patches, the signal is diffracted and scattered. The received signal on the ground has temporal fluctuations in both amplitude and phase. Either the power fading or the phase variations may lead to the loss of signal lock or increases in measurement errors. As a result, the occurrence of ionospheric scintillation is a continuity threat to a GPS receiver.

Figure 2 illustrates the impact of scintillation on the signal power of the GPS. The left plot of Figure 2 portrays a healthy GPS signal-to-noise power ratio. Typical healthy signals usually range between 40 and 50 dB-Hz.

However, if ionospheric scintillation occurs, at some moments, we have deep power fades up to 20 dB or more. As you can see in the right plot of Figure 2, during a period of 90 seconds, there are 10 power fades of up to 20 dB or more. The signal level during these deep power fades is below the receiver tracking threshold.

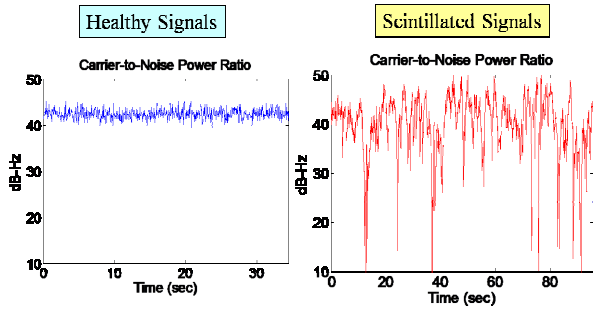

Figure 2: GPS signal-to-Noise Power Ratio for Healthy and Scintillated Signals

2.1.1 Construct Ionospheric Scintillation Effects on GPS RF Signals

To evaluate the performance of the designed GPS receiver under scintillation condition, we construct the scintillation effects on GPS signals using the Spirent 7700 GPS constellation simulator (courtesy of SiRF Inc.). The healthy GPS RF signals can easily be generated by the simulator. Both the amplitude and the phase scintillations are added onto the healthy signals by applying external commands to the simulator.

To have high fidelity amplitude scintillation for generating the external commands, we utilize real scintillated GPS intermediate frequency (IF) data provided by Air Force Research Lab (AFRL). The scintillated GPS IF data were collected on Ascension Island in 2001 (Figure 3).

Figure 3: Scintillated GPS Data Collection on Ascension Island, 2001

The profile of the amplitude scintillation (the right plot of Figure 2) is extracted using a NordNav software receiver to process the scintillated GPS IF data. Furthermore, this amplitude profile is applied as the external commands to dither the original healthy GPS signals. Each simulated channel is one-to-one mapped to the real scintillated GPS channels. As a result, we have built a realistic amplitude scintillation scenario in the GPS simulator based on real data.

In addition to the amplitude scintillation, we also consider the phase scintillation effects on GPS signals. Since the phase of the real scintillated GPS data cannot be tracked due to the deep power fading, we cannot obtain the phase scintillation directly from the real data. Instead, we generate the profile of the phase scintillation based on the most widely accepted inverse power law model of phase scintillation [2]. Likewise, this phase scintillation is applied as the external commands to dither the original healthy phase generated in the simulator.

With the aforementioned implementations, we obtain GPS RF signals with realistic scintillation effects.

2.2 Impacts of Aircraft Vibration on a Crystal Oscillator

A GPS receiver must generate a replica GPS signal to track the received GPS signal. The quality of the replica signal depends on the stability of the local oscillator. A low-cost GPS receiver usually uses a crystal oscillator for the timing function. The stability of an oscillator can be characterized by the phase-noise power spectrum density (PSD). Figure 4 depicts the generic phase-noise PSD of a typical temperature-compensated crystal oscillator (TCXO) [3]. The measured data in Figure 4 originate from the clock frequency measurements provided by the designed GPS software receiver (Section 3). The details of deriving the model of the clock phase noise are provided in [4]. Note that the phase offset in the replica signal due to the phase noise of oscillator must be tracked by the carrier tracking loop.

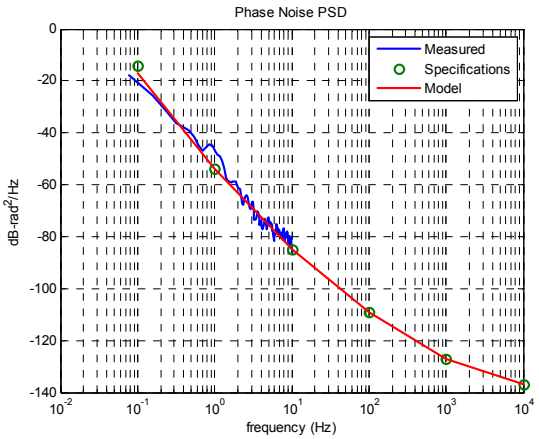

Figure 4: The Generic Phase Noise of a TCXO

However, the oscillator is sensitive to vibration. The phase noise is boosted by the aircraft's platform vibration. Figure 5 describes the vibration-affected phase-noise PSD. For the considered TCXO under the aircraft vibration condition represented in Figure 5, the maximum increase in the phase-noise PSD floor is 6 dB. The analysis of this vibration impact on the stability of an oscillator can be found in [4]. This additional phase noise due to the platform vibration also demands a higher bandwidth for the GPS receiver.

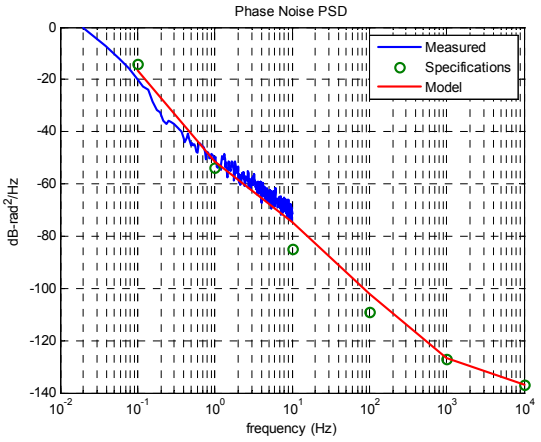

Figure 5: The Vibration-affected Phase Noise of a TCXO

The measured position error due to the overall clock dynamics (Figure 5) is plotted as a function of time in Figure 6. From Figure 6, we learn that the clock error exceeds one wave length of the GPS L1 carrier within 1 second.

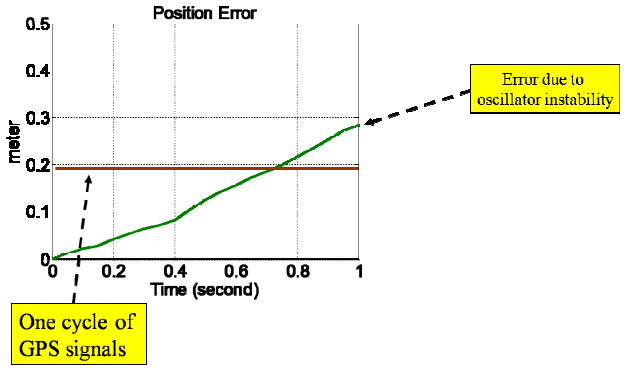

Figure 6: The Position Error Due to the Clock Dynamics of a TCXO in an Aircraft Vibration Environment

2.2.1 Construct Vibration-affected Clock Signals

To obtain the vibration effects on the oscillator, we utilize a clock emulator (courtesy of SiRF Inc.) to generate the vibration affected clock signals.

The front-end used to collect GPS RF data from the Spirent simulator can be driven by an external clock. We use the clock emulator as the external clock. The clock emulator itself is a high-quality clock with low phase noise (Agilent E4424B). It can generate an arbitrary waveform to emulate the defects of an inexpensive crystal oscillator in the following three ways:

1. Specify points of the desired phase noise density in the frequency domain;
2. Specify points of the desired discrete spurious signals in the frequency domain, and
3. Emulate thermal perturbations as a function of time.

We use method 1 to generate the clock signal with desired phase noise PSD in Figure 5. The measured PSD in Figure 5 is the clock phase error measured by our GPS software receiver. The model (red curve) in Figure 5 is the desired phase PSD programmed into the clock emulator. From Figure 5, we confirm that the clock signal truly represents the behavior of the clock when it is on-board a vibrating aircraft.

2.3 Aircraft Platform Dynamics

The third challenge is the dynamics stress due to the maneuvers of the aircraft. The actual flight path of an aircraft is not as smooth as the straight path portrayed in Figure 7. There are disturbances, wind gusts, and pilot maneuvers. In [5], it requires a GPS receiver to continuously operate when the platform is subject to an acceleration of 0.58 g or a jerk of 0.25 g/sec, where g is the gravity, 9.8 m/sec^2.

Figure 7 illustrates the position error due to the acceleration and the jerk, respectively. If the GPS receiver does not track the platform dynamics, the position error increases rapidly. Therefore, to overcome the dynamic stress, the GPS receiver demands a higher bandwidth.

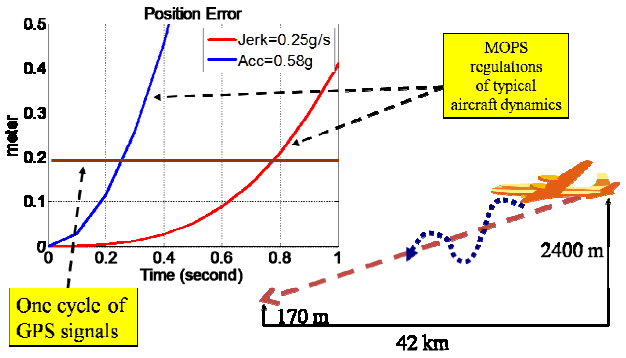

Figure 7: Aircraft Platform Dynamics

We have considered this platform dynamics in the linear model analysis to determine the optimal bandwidth (Section 4). Since we are applying Doppler-aiding to the carrier tracking loop of the GPS receiver, the platform dynamics are removed by the Doppler-aiding. Therefore, we only construct the nominal aircraft landing dynamics in the Spirent simulator. This setup is reasonable because once the bandwidth of the un-aided GPS receiver is large enough; the tracking error due to platform dynamics is very small. When the Doppler-aiding is applied, the platform dynamics are tracked by the inertial system. Hence, the dominant error in a low bandwidth is the clock dynamics.

3. DOPPLER-AIDED GPS RECEIVER

The main idea to resolve the scintillation problem is to find the aiding source, which allows us to reduce the receiver bandwidth. In this work, we consider two Doppler-aiding sources: vector processing [1] and an inertial system. Vector processing calculates the Doppler estimate of the weak channels using the strong channels. This aiding method is effective when there are at least four or more strong channels. However, if there are fewer than four healthy channels, the Doppler estimate must rely on an external measurement-, an inertial system. The Doppler-aiding using an inertial system is achieved by tightly coupling the GPS receiver with the inertial measurement unit (IMU). In addition to the two Doppler aiding sources, we also evaluate the performance of applying Doppler aiding to both coherent and non-coherent carrier tracking loops.

3.1 The Overall Architecture

Figure 8 demonstrates the architecture of the Doppler-aided GPS receiver that we develop in this work. The receiver runs coherent and non-coherent carrier tracking in parallel. Depending on the availability of pseudorange measurements, the navigation function switches between the two tracking modes to calculate the position, the velocity, and the time (PVT). The bit and frame synchronization of the non-coherent tracking is provided by the coherent tracking channels.

Coherent tracking means that the receiver utilizes a phase-locked loop to track the phase of the received GPS signal. In contrast, non-coherent tracking refers to the utilization of a frequency-locked loop to track the frequency of the received GPS signal.

To apply Doppler aiding to both carrier tracking loop, the function of channel Doppler estimation is developed (Figure 8). This Doppler estimate function is synchronized to each channel according to the navigation data bit boundary of each channel. This Doppler estimate function utilizes the two inputs to calculate the channel Doppler frequencies. The first input is the PVT of the satellite and the second input is the PVT of the receiver.

The satellite's PVT information is obtained from the navigation data at the beginning of the tracking process.

The PVT of the receiver is from either the vector processing or tightly coupling the GPS with the IMU. Using vector processing requires at least four healthy satellites. We implement this technique to validate the effectiveness under the strong scintillation condition.

However, if there fewer than four healthy channels, the receiver uses the Doppler estimates by tightly coupling the GPS with the IMU. As illustrated in Figure 8, the IMU measures accelerations and platform angular rates. These inertial measurements are fed into the function of navigation and filtering algorithms [6] combined with the measurements of the pseudorange as well as the pseudorange rate from the GPS receiver. The output of this blending function is the best estimated PVT of the receiver. This PVT is then fed into the function of channel Doppler estimation to calculate the Doppler frequency of each channel.

In this work, the tightly-coupled GPS/INS is simulated by applying noise to the reference Doppler provided by the Spirent simulator. The quality of the simulated Doppler estimate is designed to represent the use of the automotive grade IMU that is defined quantitatively in [7].

By applying this technique, the bandwidth of the carrier tracking loops can be reduced, such that much more radio interference is tolerated by the GPS receiver. Section 4 quantitatively evaluates the performance of the technique of tightly-coupled GPS/INS.

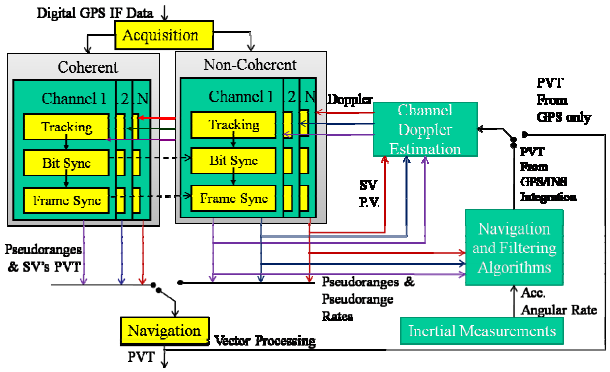

Figure 8: Doppler-Aided GPS Receiver

4. MODEL RESULTS

This section presents the designed parameters of the Doppler-aided GPS receiver illustrated in Figure 8. The two key parameters of the carrier tracking loop are the loop noise bandwidth and the pre-detection integration time (PDI). To be more capable of noise rejection, a GPS receiver needs a longer PDI. However, because of the presence of the navigation data bits in the current GPS L1 signal, the maximum value of PDI is limited to 20 ms for coherent tracking and 10 ms for non-coherent tracking [8]. Given the PDI, the loop noise bandwidth is the parameter for the carrier tracking loop designer. We prefer the noise bandwidth to be as low as possible for better noise rejection. However, the gain of the reducing bandwidth comes with a limitation. We cannot continually reduce the bandwidth. This issue leads to the discussion of the trade-off study for the bandwidth in Section 4.1.

4.1 Trade-off study for the Optimal Bandwidth

Figure 9 exemplifies the concept of designing the loop bandwidth to obtain a smaller frequency error in the non-coherent carrier tracking loop. The red line represents the frequency error due to thermal noise and the amplitude scintillation, whereas the blue line indicates the frequency error due to dynamics and the phase scintillation. As can be seen in Figure 9, some of the gain obtained from the red line by reducing the loop bandwidth is consumed by the blue line as the bandwidth becomes narrower.

The idea of Doppler-aiding is to shift the blue line as low as possible by removing the platform dynamics. When the platform dynamics are removed, a lower loop bandwidth can be applied in the carrier tracking loop. Furthermore, the clock dynamics start to dominant the frequency or phase error when Doppler-aiding is implemented. Note that the phase scintillation also causes comparable phase errors like a TCXO. Therefore, the clock dynamics and the phase scintillation prevent the reduction of the loop bandwidth. For every combination of the red and blue lines, there is an optimal loop bandwidth. The details of determining the optimal bandwidth were revealed in [4]. In subsections 4.2 and 4.3, we present the final results of the trade-off study for coherent and non-coherent tracking loops, respectively.

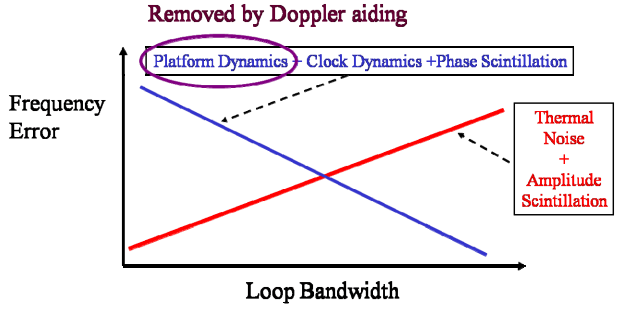

Figure 9: The trade-off study of Loop Bandwidth

4.2 Bandwidth versus C/N0 Contour for Coherent Tracking

In this subsection, we discuss the optimal bandwidth of the coherent carrier tracking loop. Figure 10 demonstrates the contour of feasible bandwidth under conditions of the carrier-to-noise power ratio (C/N0). The boundary of the contour represents the tracking threshold. Any combination of bandwidth and C/N0 within the contour indicates that the phase-locked is achieved. The region of phase-locked is defined as the *feasible* region. It is preferred that the feasible region is as large as possible. The optimal bandwidth via the model analysis is represented at the lower-left corner of the contour. From Figure 10, we discover that there is a gain of 3 dB by applying Doppler-aiding to a coherent tracking architecture under conditions including strong amplitude scintillation, phase scintillation, aircraft dynamics, and aircraft vibration affected TCXO. The lowest allowable CN0 for these conditions with Doppler aiding is 30 dB-Hz.

This high C/N0 indicates that the Doppler-aided coherent carrier tracking is not robustness to strong scintillation. Note that the clock is TCXO and the IMU is an automotive grade IMU. An expensive solution for Doppler-aided coherent tracking is not the focus in this work.

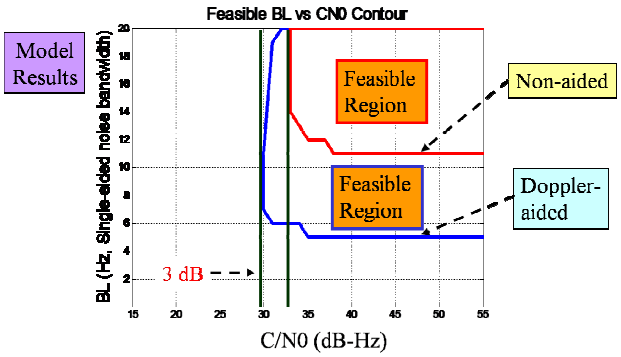

Figure 10: Bandwidth versus C/N0 Contour for Coherent Tracking

4.3 Bandwidth versus C/N0 Contour for Non-Coherent Tracking

In contrast to the coherent tracking, the Doppler-aided non-coherent tracking architecture has a gain of 6 dB (Figure 11). We can reduce the bandwidth of the frequency-locked loop from 1 Hz down to 0.2 Hz. The lowest allowable C/N0 is 22 dB-Hz. As will be seen in Section 6, Doppler-aided non-coherent tracking loop is robust to the conditions considered.

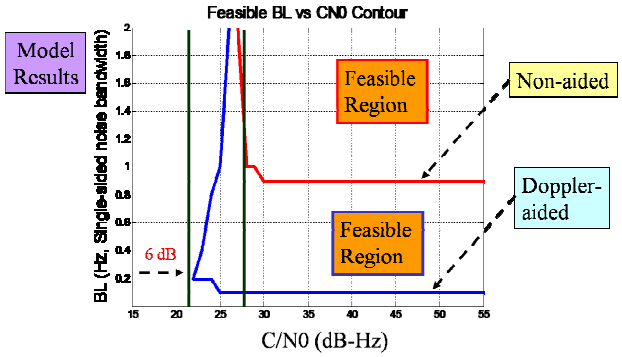

Figure 11: Bandwidth versus C/N0 Contour for Non-Coherent Tracking

5. DATA COLLECTION

Thus far, we have covered steps to build high-fidelity GPS RF signals including scintillations, platform dynamics, vibration-affected TCXO. In this section, we demonstrate the overall experimental setup.

Figure 12 portrays the flow diagram of collecting the GPS RF signals. The scenario of aircraft landing using GPS in equatorial regions is created in the Spirent simulator. The scintillation commands are used to modify the amplitude and the phase of the healthy signals in the simulator. At the output of the simulator, the scintillated GPS RF signals are generated. The GPS RF signals are then collected using the NordNav front-end to store the IF data. The NordNav front-end utilizes external clock signals to generate the replica GPS signals. The external clock is the aforementioned clock emulator. The vibration-affected TCXO clock signal is generated using the clock emulator. With this experimental setup, a realistic scenario for aircraft landing using GPS under strong scintillation condition is created.

Note that there is an assumption in the scenario. The GPS RF signals are designed to be healthy for the first two minutes. Scintillation occurs at the beginning of the third minute and lasts for seven minutes. With this setup, the navigation data bits are decoded within the first two minutes. Furthermore, this arrangement allows us to focus on the performance of carrier tracking during the period of strong scintillation. The analysis of bit error rate (BER) is future work.

The collected IF data are then processed by the designed GPS software receiver for testing performance of various combinations of Doppler-aiding sources and tracking architectures (Figure 8).

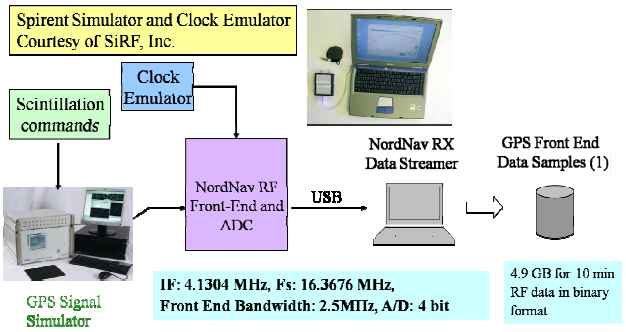

Figure 12: The Flow Diagram of Data Collection

6. EXPERIMENTAL RESULTS

The performance of the designed receiver is evaluated based on the RMS-smoothed code pseudorange measurement. Figure 13 defines the metric that we use for comparison. In this work, the target smoothed code pseudorange error is 0.36 meter. This is the RMS value including only the residual thermal noise. The bias due to clock dynamics must be removed.

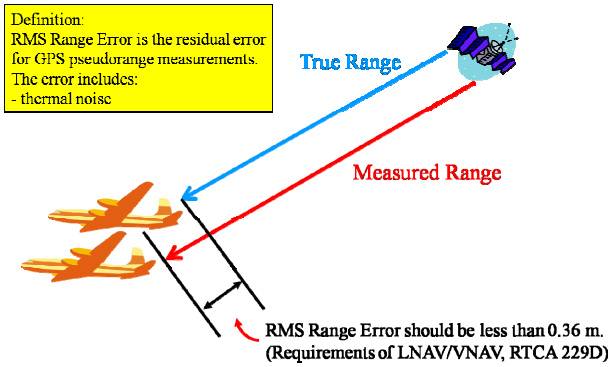

Figure 13: The RMS Smoothed Pseudorange Error

Figures 14 and 15 illustrate the profile of the power fading for the channel that we will present the RMS range error.

Figure 16 reveals the results of RMS error for various tracking architectures. From Figure 16, we see that the unaided coherent tracking loop cannot operate continuously during this strong scintillation. The jumps of the blue curve indicate cycle slips during deep power fading. The performance of the unaided non-coherent tracking loop is better than the unaided coherent tracking loop. However, the RMS value is larger than the requirement. In addition, we have noticed that the unaided non-coherent also lost frequency lock at a few deep power fading moments.

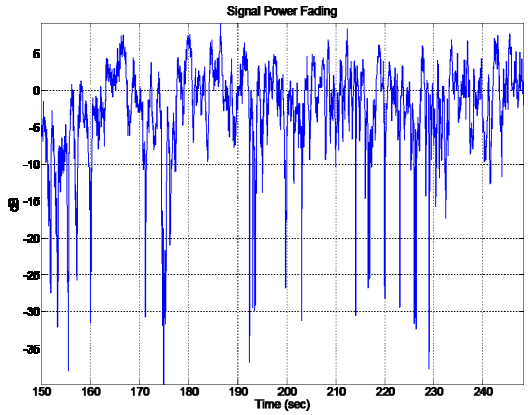

Figure 14: The Profile of Signal Power Fading

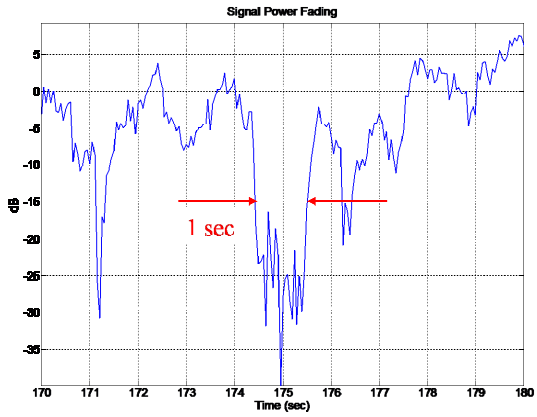

Figure 15: The Profile of Signal Power Fading (Zoomed in)

After applying those two Doppler-aiding techniques to the non-coherent tracking loop, the pink and the red curves in Figure 16 demonstrate the effectiveness of Doppler-aiding.

Figure 17 presents the vertical error and velocity error of Doppler-aided non-coherent tracking architecture. In Figure 17, there are 7 channels, 5 of which are affected by scintillation. In Figure 17, we demonstrate that the receiver does not drop any channel during moments of deep power fading. This means that the receiver operates continuously without losing the satellite geometry.

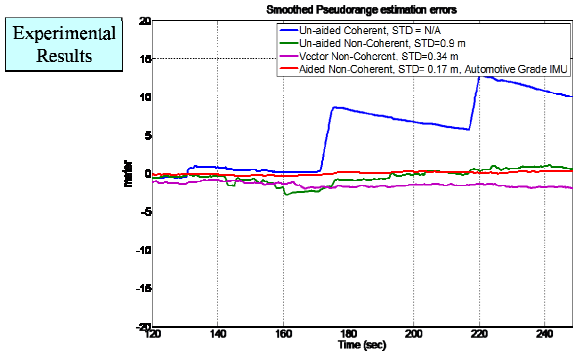

Figure 16: The Smoothed Pseudo-range Error

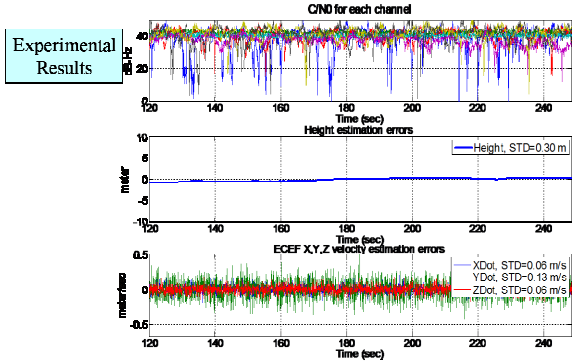

Figure 17: Vertical and Velocity Errors

7. CONCLUSIONS AND FUTURE WORK

We have built a realistic channel model for aircraft landing under scintillation conditions. We have demonstrated that a Doppler-aided non-coherent tracking loop can provide continuous operation with the required pseudo-range accuracy under strong scintillation conditions. Two effective Doppler aiding sources have been tested:

– Vector Processing
– Tightly coupled of GPS and automotive grade INS

For the future work, the bit error rate (BER) using Doppler-aided non-coherent tracking architecture requires further investigation.

ACKNOWLEDGMENTS

The authors gratefully acknowledge the support of the FAA CRDA 08-G-007.

We are sincerely grateful to Dan Babitch, SiRF, San Jose, for providing the clock emulator and data from the Spirent simulator and especially for his comprehensive

efforts in generating the emulated phase noise for a vibrating oscillator. Special thanks go to Dr. Ted Beach, AFRL for providing us with the real scintillated GPS raw IF data collected from Ascension Island in 2001; to Paul Crampton, Spirent Inc. for his enormous help in creating the scintillation scenario as well as logging data from the Spirent 7700 GPS constellation simulator.

REFERENCES

1. Spilker, J.J. and et al., *Global Positioning System: Theory and Applications, Vol. 1, AIAA, Washington, DC, 1996*.
2. Morrissey, T.N., Shallberg, K.W., and et al, "GPS Receiver Performance Characterization Under Simulated Ionospheric Scintillation Environments," *Proc. ION AM 2000*, pp. 577-587.
3. Spilker, J., Digital Communication by Satellite, *Prentice-Hall, Cambridge, Massachusetts*, pp. 336-397, 1977
4. Chiou, T.Y., "Model Analysis on the Performance for an Inertial Aided FLL-Assisted-PLL Carrier-Tracking Loop in the Presence of Ionospheric Scintillation," *Proc. ION NTM 2007*, pp. 2895-2910.
5. RTCA, Minimum Operational Performance Standards for Sensors Using GPS/WAAS, *RTCA Document No. RTCA/DO-229*, January 1996.
6. R.G. Brown and P.Y.C. Hwang, *Introduction to Random Signals and Applied Kalman Filtering with Matlab Exercises and Solutions, 3rd Edition*, Wiley, 1996.
7. Gebre-Egziabher, D., Design and Performance Analysis of a Low-Cost Aided Dead Reckoning Navigator, *Ph.D. Thesis, Stanford University, Stanford, California, U.S.A.*, December, 2001.
8. Van Dierendonck, A.J., "GPS Receivers," in *Global Positioning System: Theory and Applications, Vol. 1, AIAA, Washington, DC, 1996*, pp. 330-433.